Available online at www.sciencedirect.com
ScienceDirect
Journal of Colloid and Interface Science 316 (2007) 796–802
JOURNAL OF Colloid and Interface Science
www.elsevier.com/locate/jcis

Stopped-flow kinetic studies of sphere-to-rod transitions of sodium alkyl sulfate micelles induced by hydrotropic salt

Jingyan Zhang [a], Zhishen Ge [a], Xiaoze Jiang [a], P.A. Hassan [b], Shiyong Liu [a,*]

[a] *Department of Polymer Science and Engineering, Hefei National Laboratory for Physical Sciences at the Microscale, University of Science and Technology of China, Hefei, Anhui 230026, China*
[b] *Novel Materials and Structural Chemistry Division, Bhabha Atomic Research Center, Mumbai 400 085, India*

Received 31 May 2007; accepted 30 August 2007
Available online 4 September 2007

Abstract

The kinetics and mechanism of sphere-to-rod transitions of sodium alkyl sulfate micelles induced by hydrotropic salt, *p*-toluidine hydrochloride (PTHC), were investigated by stopped-flow with light scattering detection. Spherical sodium dodecyl sulfate (SDS) micelles transform into short ellipsoidal shapes at low salt concentrations ([PTHC]/[SDS], $\chi_{PTHC} = 0.3$ and 0.4). Upon stopped-flow mixing aqueous solutions of spherical SDS micelles with PTHC, the scattered light intensity gradually increases with time. Single exponential fitting of the dynamic traces leads to characteristic relaxation time, τ_g, for the growth process from spherical to ellipsoidal micelles, and it increases with increasing SDS concentrations. This suggests that ellipsoidal micelles might be produced by successive insertion of unimers into spherical micelles, similar to the case of formation of spherical micelles as suggested by Aniansson–Wall (A–W) theory. At $\chi_{PTHC} \geqslant 0.5$, rod-like micelles with much higher axial ratio form. The scattered light intensity exhibits an initially abrupt increase and then levels off. The dynamic curves can be well fitted with single exponential functions, and the obtained τ_g decreases with increasing SDS concentration. Thus, the growth from spherical to rod-like micelles might proceed via fusion of spherical micelles, in agreement with mechanism proposed by Ikeda et al. At $\chi_{PTHC} = 0.3$ and 0.6, the apparent activation energies obtained from temperature dependent kinetic studies for the micellar growth are 40.4 and 3.6 kJ/mol, respectively. The large differences between activation energies for the growth from spherical to ellipsoidal micelles at low χ_{PTHC} and the sphere-to-rod transition at high χ_{PTHC} further indicate that they should follow different mechanisms. Moreover, the sphere-to-rod transition kinetics of sodium alkyl sulfate with varying hydrophobic chain lengths ($n = 10$, 12, 14, and 16) are also studied. The longer the carbon chain lengths, the slower the sphere-to-rod transition.

Keywords: Sphere-to-rod transition; Rod-like micelles; Stopped-flow; Kinetics; Hydrotropic salt

1. Introduction

Amphiphilic molecules can form spherical aggregates in aqueous solution above the critical micellization concentration (cmc) [1–4]. Spherical micelles may grow in size and change their shape, resulting in the formation of ellipsoidal, rod-like, or even long flexible micelles depending on the nature of the surfactant molecule, concentration, temperature, pressure, and additives such as short-chain alcohols or salts [5–13]. It has been well known that the addition of electrolytes to an ionic surfactant solution above the cmc can facilitate the transition from spherical to rod-like micelles by screening the electrostatic repulsions between the charged headgroups [14]. When the micellar length becomes larger than the persistence length, the micelles possess a worm-like shape [7,15]. Compared to inorganic salts (e.g., NaCl, KBr) [7–9,16,17], which bind moderately to ionic surfactant micelles and lead to gradual micellar growth, organic salts (e.g., salicylate, *p*-toluene sulfonate) can bind strongly to the micellar surface and efficiently promote the transition from spherical micelles to rod-like or even worm-like micelles at significantly lower salt contents [18–22]. Therefore, this special type of organic salts is also termed as hydrotropes or hydrotropic salts [23], they are weakly surface-active and

* Corresponding author.
E-mail address: sliu@ustc.edu.cn (S. Liu).

0021-9797/$ – see front matter
doi:10.1016/j.jcis.2007.08.067

can considerably increase the solubility of organic substances in aqueous solution.

Micelles are in dynamic equilibrium with individual surfactant molecules, and are continuously decomposing and reassembling [1–4]. The micellization dynamics of small molecule surfactant near the association equilibrium can be relatively well described by the Aniansson and Wall (A–W) theory [24–26]. An important assumption in the A–W theory is that all changes are due to an elementary process of insertion/expulsion of individual chains ('unimers') into/out of the micelle. Two relaxation processes are typically involved in micellar solutions. The first is a fast relaxation process (τ_1) associated with the quick exchange of unimers. τ_1 is typically on the order of microseconds for ionic surfactants. The second is a slow relaxation process (τ_2) associated with the micelle formation/breakup. The average lifetime of micelles can be calculated from τ_2, which is on the order of milliseconds to seconds [27–29].

The A–W theory predicted that both τ_1 and τ_2 are inversely proportional to the total surfactant concentrations. This has been confirmed by many experiments using classical relaxation techniques such as stopped-flow, temperature-jump, pressure-jump, and ultrasonic absorption [27–29]. However, at higher surfactant concentrations or in the presence of salt, it has been observed that τ_2 decreases with total surfactant concentration. Kahlweit and coworkers [30,31] proposed that at higher surfactant concentration, the counterion concentration also increases, which compresses the electrical double-layer surrounding the micelles and reduces charge repulsion between headgroups [2–4]. Thus, micelle fusion/fission process is favored instead of the unimer insertion/expulsion pathway. The Kahlweit theory can satisfactorily explain the surfactant concentration dependence of τ_2.

In the Aniansson's [24–26] and Kahlweit's [30,31] models, conformational changes (e.g., sphere-to-rod transition) during the micelle growth were not considered. Harada et al. [32] studied the sphere-to-rod transition of cetyltrimethylammonium bromide (CTAB) micelles using the pressure-jump technique. Similar to the two relaxations observed for spherical micelles near association equilibrium, two new relaxation processes were detected for the sphere-to-rod transition, which can be ascribed to unimer exchange (fast relaxation) and the overall formation and dissolution of rod-like micelles (slow relaxation, τ_s), respectively. They further concluded that the rod-like micelles are formed by successive association of monomers to the spherical micelles in a similar manner as spherical micelles are formed. However, a closer examination of the surfactant concentration dependence of τ_s revealed that fusion of spherical micelles may still be involved in the sphere-to-rod transition, especially at much higher surfactant concentrations.

Cates et al. [33] theoretically considered the role of micelle fusion-fission on the micellization dynamic of elongated micelles and deduced an equation describing the relationship between the relaxation time and micellar length. Using T-jump with light scattering detection, Waton et al. [34,35] measured the relaxation time associated with the fusion/fission process where the shape of micelles varies from a sphere to rod-like or worm-like for sodium dodecyl sulfate (SDS) in the presence of 0.6–1.0 mol/L NaCl, they also calculated the fusion probability and found that it increased with increasing salt concentrations.

In all the above cases, only small perturbations from the equilibrium state were involved. For large deviations from the initial state, such as the whole process of sphere-to-rod transition induced by inorganic or organic salts, the mechanism and kinetic processes has remained unexplored. Stopped-flow technique has been proved to be quite useful in determining the relaxation time associated with the micellar growth or dissociation processes [36–39]. The stopped-flow dilution technique was successfully employed to measure the average lifetime of Triton X-100 or Brij 35 micelles [28,29,40], the results were in excellent agreement with pressure-jump studies.

Hassan et al. [20,41] recently reported the equilibrium processes of sphere-to-rod transitions of SDS micelles using a combination of laser light scattering (LLS), small angle neutron scattering (SANS), viscometry, and rheological measurements. In this communication, we further employed stopped-flow light scattering to investigate the kinetics and mechanisms of the sphere-to-rod transition of SDS micelles induced by *p*-toluidine hydrochloride (PTHC). The concentration dependence of the characteristic relaxation time (τ_g) associated with micellar growth was measured at different molar ratios of PTHC to SDS (χ_{PTHC}). The transition kinetics and mechanisms were discussed in terms of the final equilibrium micelle structures. Moreover, the sphere-to-rod transition kinetics of sodium alkyl sulfate with varying carbon chain lengths ($n = 10, 12, 14, 16$) were also investigated.

2. Experimental

2.1. Materials

Sodium dodecyl sulfate (SDS) (analytical grade, Shanghai Chemical Reagent Co.) was recrystallized from anhydrous ethanol. Sodium decyl sulfate (SDeS, Acros), sodium tetradecyl sulfate (STS, Avocado), sodium hexadecyl sulfate (SHS, Alfa), and *p*-toluidine hydrochloride (PTHC, Fluka) were used without further purification. Stock solutions of sodium alkyl sulfates and PTHC were prepared in deionized water. For stopped-flow studies, all solutions prior to mixing were filtered through 0.45 μm nitrocellulose filters (Acrodisc).

2.2. Surface tensiometry

Equilibrium surface tensions were measured with a JK99B tensiometer. The instrument was calibrated against deionized water and the agreement with literature values was typically within ±0.1 mN/m. The measurements were carried out with freshly made solutions at $25.0 \pm 0.1\,^{\circ}\mathrm{C}$.

2.3. Stopped-flow with light-scattering detection

Stopped-flow studies were carried out using a Bio-Logic SFM300/S stopped-flow instrument. The SFM-300/S is a 3-syringe (10 mL) instrument in which all step-motor-driven syringes (S1, S2, S3) can be operated independently to carry out

single- or double-mixing. The SFM-300/S stopped-flow device is attached to the MOS-250 spectrometer; kinetic data were fitted using the program Biokine (Bio-Logic). For the light scattering detection at a scattering angle of 90°, both the excitation and emission wavelengths were adjusted to 335 nm with 10 nm slits. Using FC-08 or FC-15 flow cells, the typical dead times are 1.1 and 2.6 ms, respectively.

3. Results and discussion

3.1. Comparison of rates of micellar growth induced by PTHC and NaCl

Using a combination of LLS and SANS, Hassan et al. [20,41] successfully established that spherical SDS micelles can transform into short ellipsoidal shapes at low PTHC contents (i.e., [PTHC]/[SDS], $\chi_{PTHC} = 0.3$ and 0.4). At $\chi_{PTHC} \geqslant 0.5$, rod-like micelles with much higher axial ratio form. PTHC strongly binds to the surface of SDS micelles with its *meta*- and *para*-positions inserted into the micellar interior, and the *ortho*-protons and NH_4^+ group protruding from the micelle surface. Thus, there is a concomitant decrease of surface charge density of SDS micelles upon increasing χ_{PTHC}. We measured cmc values of SDS solutions at different molar ratios of PTHC to SDS using surface tensiometry (Fig. 1). In the absence of PTHC, SDS exhibits a cmc of ~8.3 mM at 25 °C. Upon addition of PTHC, the cmc of SDS solutions abruptly decreases to 1.1 and 0.75 mM at $\chi_{PTHC} = 0.3$ and 0.6, respectively. This strongly suggests that PTHC can screen the electrostatic repulsions between surfactant headgroups and favor the formation of larger aggregates [14].

It has been well known that inorganic salts such as NaCl only moderately bind to surfactant micelles and lead to gradual micellar growth [7–9,16,17]. On the other hand, organic salts such as PTHC are highly efficient in promoting micellar growth and can even induce the formation of worm-like micelles at significantly lower ratios of salt to surfactant [20,41,42]. Fig. 2 shows the time-dependence of the scattered light intensity upon stopped-flow mixing aqueous solutions of SDS with different amounts of NaCl. The final SDS concentration was fixed at 50 mM. Obviously, in the χ_{NaCl} range of 0.3–0.7, where χ_{NaCl} is the molar ratio of NaCl to SDS, all the dynamic traces exhibit relatively small positive amplitudes. The slight increase of scattered light intensity indicates that even at $\chi_{NaCl} = 0.7$, rod-like micelles did not form and spherical micelles only transform into ellipsoidal shaped ones. With increasing χ_{NaCl}, the final equilibrium scattered intensity increases moderately, indicating the formation of ellipsoidal micelles with larger aggregation numbers. This is in agreement with that obtained by Waton and Michels [34], they reported that the micellar length is larger at 1.0 M NaCl than at 0.6 M NaCl.

On the other hand, the addition of PTHC into the spherical SDS micelles results in drastically different kinetic processes (Fig. 3a). At $\chi_{PTHC} = 0.4$ and 0.45, scattered light intensity gradually increases with time. It should be noted that the relative increase is more prominent than that by NaCl at comparable salt ratios (Fig. 2). With increasing χ_{PTHC}, the micelle formation kinetics becomes apparently much faster.

All the dynamic traces at $\chi_{PTHC} \geqslant 0.5$ in Fig. 3a can be well fitted with a single exponential function. The obtained characteristic relaxation times (τ_g) were plotted in Fig. 3b as a function of χ_{PTHC}. We can clearly see that the decrease of τ_g with increasing χ_{PTHC}. The increase of sphere-to-rod transition rate with increasing χ_{PTHC} can be rationalized to the fractional charges present at the surface of micelles. PTHC strongly adsorbs into the micelle surface and screens the charge repulsion between surfactant headgroups [20,41]. The higher the PTHC concentration, the lower stability of spherical micelles due to the reduced stabilization effects of headgroups, and consequently the faster the micellar growth [14]. Using T-jump with light scattering detection, Waton and Michels [34] determined the relaxation time associated the length changes of SDS micelles induced by NaCl. At fixed SDS concentrations, the slow relaxation time constants also decreased with increasing χ_{NaCl}. They also estimated the value of potential barrier for the micelle fusion/fission process, which was $11kT$ for 0.6 M NaCl and $8kT$ for 1.0 M samples, the decreased energy barrier at increasing χ_{NaCl} could well explain the faster rate of micelle growth.

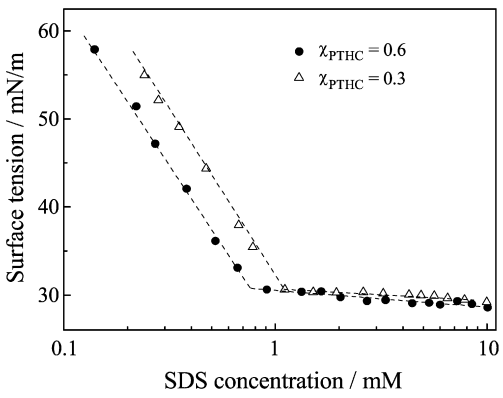

Fig. 1. Surface tensions as a function of SDS concentrations at different [PTHC]/[SDS] ratios, χ_{PTHC}, and 25 °C.

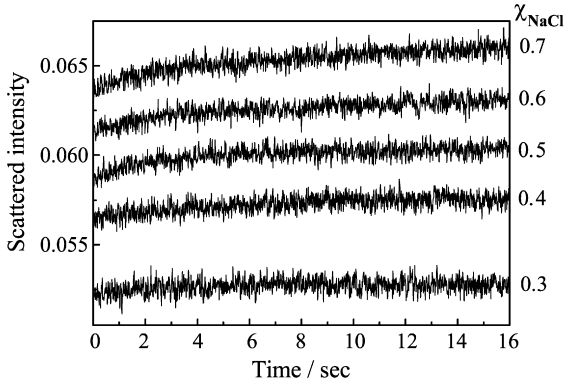

Fig. 2. Time-dependence of scattered light intensity upon stopped-flow mixing aqueous solutions of SDS with different amounts of NaCl at 25 °C. The final SDS concentration was fixed at 50 mM. χ_{NaCl} is the molar ratio of NaCl to SDS.

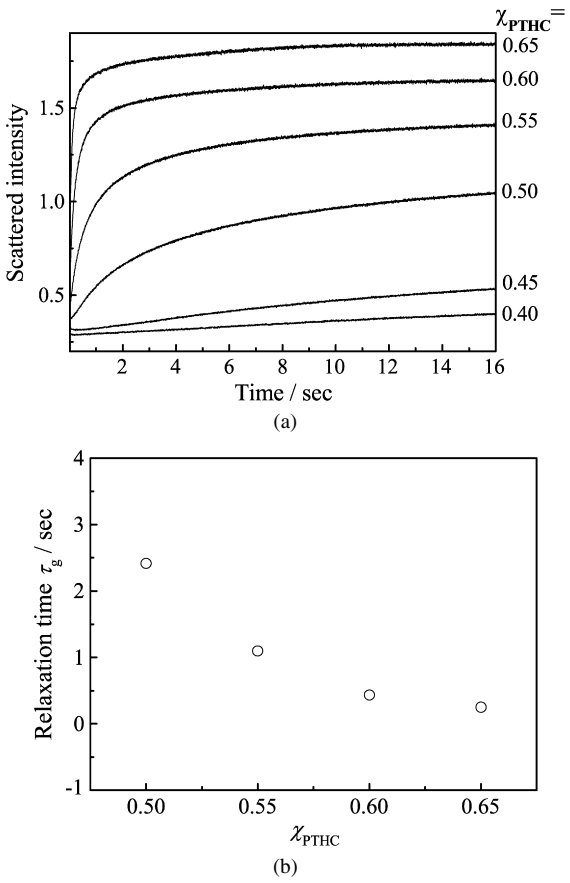

Fig. 3. (a) Time-dependence of scattered light intensity and (b) single exponential fitting results of dynamic traces upon stopped-flow mixing aqueous solutions of SDS with different amounts of PTHC at 25 °C. The final SDS concentration was fixed at 50 mM. χ_{PTHC} is the molar ratio of PTHC to SDS.

3.2. Concentration dependence of micellar growth kinetics

τ_g obtained by the stopped-flow technique can be ascribed to processes of growth from spherical to ellipsoidal micelles at low χ_{PTHC} and the sphere-to-rod transition at high χ_{PTHC} ($\geqslant$0.5). Two possible pathways exist, i.e., successive incorporation of unimers into spherical micelles or fusion of spherical micelles, similar to the case of formation of spherical micelles as proposed by Aniansson et al. [24–26] and Kahlweit et al. [30,31], respectively. The concentration dependence of τ_g at different χ_{PTHC} can be employed to differentiate the underlying mechanisms.

The scattered light intensity initially increase with time gradually, and then reach a plateau at $\chi_{PTHC} = 0.3$, suggesting that the average aggregation number, N_{agg}, of the aggregates only increases moderately. This is in agreement with the results obtained by Hassan and coworkers [20,41]; N_{agg} increases from ~79 at $\chi_{PTHC} = 0$ to ~131 at $\chi_{PTHC} = 0.3$. Compared to that at $\chi_{PTHC} = 0$, more ellipsoidal shaped micelles formed at $\chi_{PTHC} = 0.3$, with the semiminor and semimajor axis being 1.7 and 4.7 nm, respectively. Single exponential fitting results of dynamic traces obtained at different SDS concentrations and a fixed χ_{PTHC} of were shown in Fig. 4.

At a fixed χ_{PTHC} of 0.3, τ_g is in the range of 0.1–2.3 s, and it increases with increasing surfactant concentrations. Based on

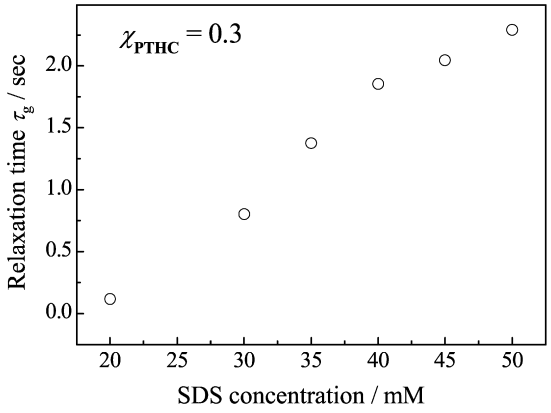

Fig. 4. Single exponential fitting results of dynamic traces obtained at different final SDS concentrations and a fixed χ_{PTHC} of 0.3. The temperature is at 25 °C.

SANS results, Hassan et al. [41] established that there was still strong repulsive interactions between the formed ellipsoidal micelles at $\chi_{PTHC} = 0.3$. Upon a jump of χ_{PTHC} from 0 to 0.3, the growth from spherical to ellipsoidal micelles should proceed via successive incorporation of unimer chains into spherical micelles, and the fusion between spherical micelles should be less favored. This was further supported by the concentration dependence of τ_g. In aqueous solutions of spherical micelles, the well-accepted A–W theory suggested that the formation/breakup of spherical micelles proceeds via the unimer entry/expulsion mechanism, and predicted that the associated τ_2 will increase with increasing surfactant concentrations [24–26].

Fig. 5a shows the time-dependence of scattered intensity obtained at different final SDS concentrations and a fixed χ_{PTHC} of 0.6. As revealed by Hassan et al. [41], the final equilibrium states are rod-like micelles with an aggregation number of ~720 and a micelle length of ~28 nm. The scattered intensity grows more dramatically and abruptly compared to that at $\chi_{PTHC} = 0.3$. We can observe that at increasing SDS concentrations, the increase of final equilibrium scattered intensity values is less prominent. This could be due to non-linear changes of dn/dC and/or the occurrence of entanglement between rod-like micelles at high SDS concentrations [15].

Apparently, the sphere-to-rod transition is much faster at higher surfactant concentrations. Fig. 5b shows the single exponential fitting results of dynamic traces. The decrease of τ_g with increasing surfactant concentrations indicates that sphere-to-rod transition upon a jump of χ_{PTHC} from 0 to 0.6 might proceed via different mechanisms compared to that at a final χ_{PTHC} of 0.3.

Ikeda et al. [13,43] theoretically proposed that the sphere-to-rod transition may also proceed via fusion of spherical micelles, suggesting that the τ_g will decrease steeply with increasing surfactant concentrations [32], which is similar to the case of formation/breakup of spherical micelles via the micelle fusion/fission mechanism as suggested by Kahlweit et al. [30,31]. Thus, the surfactant concentration dependence of τ_g as shown in Fig. 5b clearly indicates that at a final χ_{PTHC} of 0.6, the sphere-to-rod transition proceeds via the fusion of spherical micelles. This is drastically in contrast to the mechanism of growth from spherical to ellipsoidal micelles (Fig. 3b).

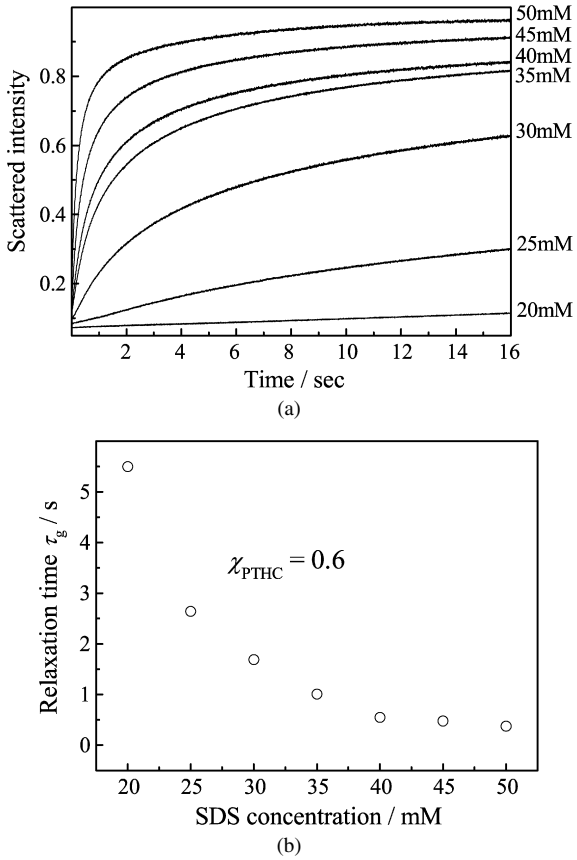

Fig. 5. (a) Time-dependence of scattered light intensity and (b) single exponential fitting results obtained at different final SDS concentrations and a fixed χ_{PTHC} of 0.6. The temperature is at 25 °C.

According to Hassan et al. [41], the fractional charge at the micelle surface decreases from 0.42 at $\chi_{PTHC} = 0$ to 0.1 at $\chi_{PTHC} = 0.6$, and the inter-micellar repulsion vanishes at $\chi_{PTHC} \geqslant 0.5$. Actually, for rod-like micelles, fusion and fission of chain segments are continuously occurring due to the absence of inter-micellar electrostatic repulsions. At the final stage of sphere-to-rod transition, the fusion rate of micelles will be equal to that of micelle fission, and the equilibrium will be established. The screening of surface charges at higher χ_{PTHC} will then render the micelle fusion/fission mechanism more plausible.

Cates et al. [33] predicted that for rod-like micelles near the association equilibrium, the slow relaxation time associated with micelle fusion/fission follows $\tau = 1/2k_b m$, where k_b is the breakup probability per unit length, and m is average length of micelles, which varies with the surfactant concentration C as $C^{1/2}$. They further verified this predication based on the T-jump results for rod-like SDS micelles. It is interesting to note that, when Fig. 5b was plotted in logarithmic scale, we indeed observed that $1/\tau_g$ scaled linearly to the total surfactant concentrations. This indicated that although τ_g was obtained from sphere-to-rod transitions by the stopped-flow technique, which represents a large deviation from the equilibrium state, the results agree quite well with those obtained from T-jump studies [28,29,40].

The strong binding of PTHC to the micelle surface compresses the electrical double layer and reduces inter-micellar charge repulsions, allowing micelles to come closer to each other such that attractive dispersion forces (i.e., van der Waals forces) lead to reversible fusion/fission coagulations [30,31]. It should be noted that micellar lengths of the final equilibrium rod-like micelles should be polydisperse in nature due to the fast fusion/fission events. In the current study, the time-dependence of scattered light intensity at 90° was monitored during the sphere-to-rod transition process, and it mainly correlates with the average aggregation number, N_{agg}, per micelle or the average lengths of rod-like micelles. Thus the effects of size polydispersity of rod-like micelles on the scattered light intensity were negligible. This partially explains the observed monotonic evolution of scattered intensity with time during the sphere-to-rod transition.

Surfactant concentration dependence of kinetics studies at other χ_{PTHC} ratios further indicate that the transformation of growth mechanisms from the incorporation of unimers into spherical micelles to the fusion of spherical micelles occurs at $\chi_{PTHC} \geqslant 0.5$. This critical value corresponds to the point where rod-like micelles with the axial ratio larger than 10 were formed [20,41].

At a final $\chi_{PTHC} > 0.65$, the spherical micelles eventually develop into long, flexible entities due to the strongly associative nature of the hydrophobic salt and surfactant [20], the mixed solution are so viscous and reliable results cannot be obtained via the stopped-flow technique.

3.3. Temperature dependence of micellar growth kinetics

Fig. 6 shows the temperature dependence of $1/\tau_g$ obtained from the micellar growth process at a final χ_{PTHC} of 0.3 and 0.6, respectively. It is quite expected that τ_g decreases with increasing temperatures, which is typically observed for other small molecule surfactants [1–4]. The Arrhenius plots in Fig. 6 yield activation energies of 40.4 and 3.6 kJ/mol for micellar growth upon jumping of χ_{PTHC} from 0 to the final values of 0.3 and 0.6, respectively. The considerable differences between activation energies for the growth from spherical to ellipsoidal micelles at low χ_{PTHC} and the sphere-to-rod transition at high χ_{PTHC} further indicate that they should follow different mechanisms. The large apparent activation energy obtained for the former can be reasonably explained considering that the transition involves the successive incorporation of unimer chains into spherical micelles. For the formation of spherical micelles of surfactants, it has been established that the activation energy for the micelle formation/breakup via the stepwise association/dissociation mechanism is much larger than that via the micelle fusion/fission one [44]. The decrease of activation energies for the micellar growth at increasing χ_{PTHC} also indicates that micelle fusion/fission becomes much easier due to decreased inter-micellar charge repulsion, leading to faster growth rate upon increasing χ_{PTHC} (Fig. 3).

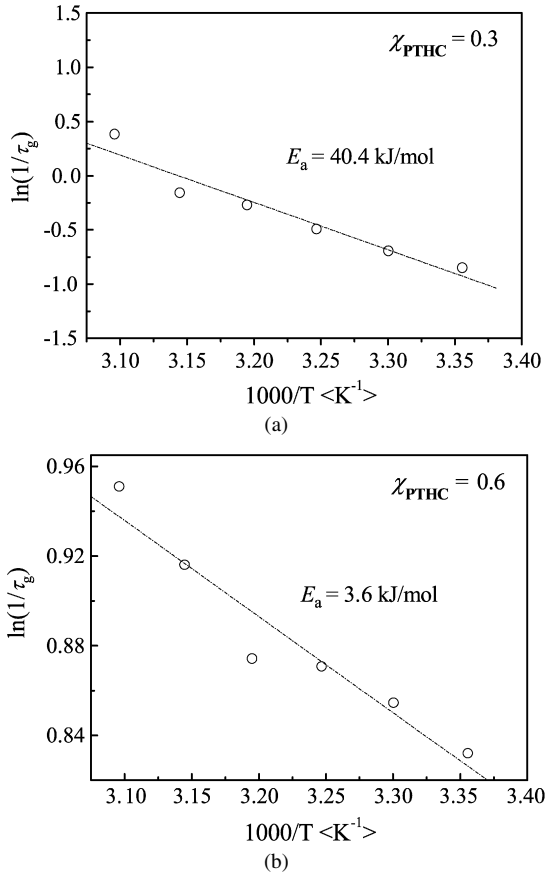

Fig. 6. Arrhenius plots of τ_g obtained for the growth of SDS micelles at (a) $\chi_{PTHC} = 0.3$ and (b) $\chi_{PTHC} = 0.6$. The final SDS concentration was fixed at 50 mM.

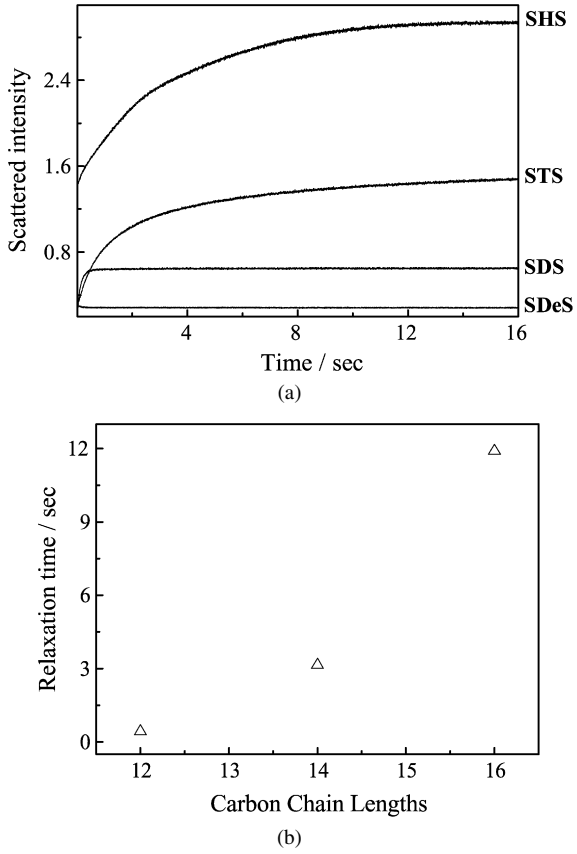

Fig. 7. (a) Time-dependence of scattered light intensity and (b) single exponential fitting results obtained for the sphere-to-rod transition of sodium alkyl sulfates with varying carbon chain lengths at 25 °C. The final surfactant concentration was 50 mM and the molar ratios of PTHC to sodium alkyl sulfates, χ_{PTHC}, were fixed at 0.6.

3.4. Sphere-to-rod transition kinetics for sodium alkyl sulfates with varying carbon chain lengths

The sphere-to-rod transition kinetics of sodium alkyl sulfates with varying chain lengths at a fixed χ_{PTHC} of 0.6 was shown in Fig. 7a and the single exponential fitting results were shown in Fig. 7b. For SDeS, we only observe small negative amplitude. As the final equilibrium value of scattered light intensity after stopped-flow mixing is larger than that of the initial solution considering the dilution effects, the micelle growth should be very fast and complete within the stopped-flow dead time (2–3 ms). Previously, we studied the sphere-to-rod transition kinetics of 4-(8-methacryloyloxyoctyl)oxybenzene sulfonate (MOBS) induced by PTHC, we also did not observe any relaxation process with positive amplitude [45]. With increasing carbon chain lengths ($n = 12$, 14, 16), we can clearly observe the micellar growth kinetics (Fig. 7a). Apparently, the longer the carbon chain length, the slower the growth rate (Fig. 7b). The slower sphere-to-rod transition kinetics for surfactants with longer carbon chain lengths should be ascribed to the increase of N_{agg} per rod-like micelle [24–26,30,31]. More effective micelle fusion/fission steps are needed for the growth from spherical micelles into longer rod-like micelles. Moreover, micelles of shorter chain surfactants are more loosely packed due to smaller van der Waals attractive forces and less hydrophobic effects. Thus, the micelle fusion/fission process of short chain surfactants only needs to encounter lower energy barriers, as compared to longer ones [28,29].

4. Conclusion

The stopped-flow technique was applied to probe the growth kinetics of SDS micelles induced by the addition of hydrotropic salt, PTHC. Spherical SDS micelles grow into ellipsoidal micelles at low $\chi_{PTHC}(\leqslant 0.4)$ or rod-like micelles at high χ_{PTHC} values ($\geqslant 0.5$). Both the surfactant concentration and temperature dependences of the obtained characteristic relaxation times, τ_g, of the micellar growth processes revealed that the spherical to ellipsoidal micelle transition and sphere-to-rod transition follow drastically different kinetic mechanisms, being the successive incorporation of unimer chains into spherical micelles and the fusion of spherical micelles, respectively. The carbon chain lengths of sodium alkyl sulfates also dramatically affect the sphere-to-rod transitions kinetics. To the best of our knowledge, this represents the first systematic investigation of micellar growth kinetics of surfactants, which involves conformational changes of micelles (sphere-to-ellipsoid, sphere-to-rod transitions) and monitors the whole transition process (i.e., accompanied with large deviations from the equilibrium states). Currently, we are employing the stopped-flow technique

to detect kinetics of the reverse process, i.e., rod-to-sphere and ellipsoid-to-sphere transitions.

Acknowledgments

This work was financially supported by an Outstanding Youth Fund (50425310) and research grants (20534020, 20674079) from the National Natural Scientific Foundation of China (NNSFC), and the "Bai Ren" Project of the Chinese Academy of Sciences.

References

[1] V. Degiorgio, M. Corti, Physics of Amphiphiles: Micelles, Vesicles, and Microemulsions, North-Holland, Amsterdam, 1985.
[2] B. Jonsson, B. Lindman, K. Holmberg, B. Kronberg, Surfactants and Polymers in Aqueous Solutions, Wiley, New York, 1998.
[3] D.F. Evans, H. Wennerstrom, The Colloidal Domain: Where Physics, Chemistry, Biology, and Technology Meet, VCH, New York, 1994.
[4] R. Zana, Surfactant Solutions: New Methods of Investigation, Dekker, New York, 1987.
[5] V.K. Aswal, P.S. Goyal, Phys. Rev. E 61 (2000) 2947–2953.
[6] L.J. Magid, Z. Li, P.D. Butler, Langmuir 16 (2000) 10028–10036.
[7] F. Kern, P. Lemarechal, S.J. Candau, M.E. Cates, Langmuir 8 (1992) 437–440.
[8] N.A. Mazer, G.B. Benedek, J. Phys. Chem. 80 (1975) 1075–1085.
[9] G. Porte, J. Appell, J. Phys. Chem. 85 (1981) 2511–2519.
[10] Kabir-ud-Din, S.L. David, S. Kumar, J. Chem. Eng. Data 42 (1997) 1224–1226.
[11] G.B. Dutt, Langmuir 21 (2005) 10391–10397.
[12] H. Heerklotz, A. Tsamaloukas, K. Kita-Tokarczyk, P. Strunz, T. Gutberlet, J. Am. Chem. Soc. 126 (2004) 16544–16552.
[13] S. Hayashi, S. Ikeda, J. Phys. Chem. 84 (1980) 744–751.
[14] J.N. Israelachvili, D.J. Mitchell, B.W. Ninham, J. Chem. Soc. Faraday Trans. 72 (1976) 1525.
[15] M.E. Cates, S.J. Candau, J. Phys. Condens. Matter 2 (1990) 6869–6892.
[16] T. Imae, S. Ikeda, J. Phys. Chem. 90 (1986) 5216–5223.
[17] P.J. Missel, N.A. Mazer, G.B. Bernedek, C.Y. Young, J. Phys. Chem. 84 (1980) 1044–1057.
[18] H. Rehage, H. Hoffman, J. Phys. Chem. 92 (1988) 4712.
[19] A. Ait Ali, R. Makhloufi, Phys. Rev. E 56 (1997) 4474.
[20] P.A. Hassan, S.R. Raghavan, E.W. Kaler, Langmuir 18 (2002) 2543–2548.
[21] R.T. Buwalda, M.C.A. Stuart, J.B.F.N. Engberts, Langmuir 16 (2000) 6780–6786.
[22] Y. Geng, L.S. Romsted, S. Froehner, D. Zanette, L.J. Magid, I.M. Cuccovia, H. Chaimovich, Langmuir 21 (2005) 562–568.
[23] D. Balasubramanian, V. Srinivas, V.G. Gaikar, M.M. Sharma, J. Phys. Chem. 93 (1989) 3865.
[24] E.A.G. Aniansson, S.N. Wall, J. Phys. Chem. 79 (1975) 857–858.
[25] E.A.G. Aniansson, S.N. Wall, M. Almgren, H. Hoffmann, I. Kielmann, W. Ulbricht, R. Zana, J. Lang, C. Tondre, J. Phys. Chem. 80 (1976) 905–922.
[26] E.A.G. Aniansson, S.N. Wall, J. Phys. Chem. 78 (1974) 1024–1032.
[27] B.A. Noskov, Adv. Colloid Interface Sci. 95 (2002) 237–293.
[28] A. Patist, J.R. Kanicky, P.K. Shukla, D.O. Shah, J. Colloid Interface Sci. 245 (2002) 1–15.
[29] A. Patist, S.G. Oh, R. Leung, D.O. Shah, Colloids Surf. A Physicochem. Eng. Asp. 176 (2001) 3–16.
[30] M. Kahlweit, J. Colloid Interface Sci. 90 (1982) 92–99.
[31] E. Lessner, M. Teubner, M. Kahlweit, J. Phys. Chem. 85 (1981) 1529–1536.
[32] S. Harada, N. Fujita, T. Sano, J. Am. Chem. Soc. 110 (1988) 8710–8711.
[33] M.S. Turner, M.E. Cates, J. Phys. France 51 (1990) 307–316.
[34] B. Michels, G. Waton, J. Phys. Chem. B 104 (2000) 228–232.
[35] G. Waton, J. Phys. Chem. B 101 (1997) 9727–9731.
[36] J. Eastoe, J.S. Dalton, A. Downer, G. Jones, D. Clarke, Langmuir 14 (1998) 1937–1939.
[37] M. Gradzielski, Curr. Opin. Colloid Interface Sci. 8 (2003) 337–345.
[38] M. Hilczer, A.V. Barzykin, M. Tachiya, Langmuir 17 (2001) 4196–4201.
[39] P.V. Yushmanov, I. Furo, P. Stilbs, Langmuir 22 (2006) 2002–2004.
[40] T. Yasunaga, K. Takeda, A.S. Harada, J. Colloid Interface Sci. 42 (1972) 457–463.
[41] P.A. Hassan, G. Fritz, E.W. Kaler, J. Colloid Interface Sci. 257 (2003) 154–162.
[42] P.A. Hassan, J.V. Yakhmi, Langmuir 16 (2000) 7187–7191.
[43] S. Ozeki, S. Ikeda, J. Colloid Interface Sci. 87 (1982) 424.
[44] C. Tondre, R. Zana, J. Colloid Interface Sci. 66 (1978) 544.
[45] Z.Y. Zhu, Y.I. Gonzalez, H.X. Xu, E.W. Kaler, S.Y. Liu, Langmuir 22 (2006) 949–955.